

mTOR Pathway Somatic Pathogenic Variants in Focal Malformations of Cortical Development

Novel Variants, Topographic Mapping, and Clinical Outcomes

Eric Krochmalnek, MSc,* Andrea Accogli, MD,* Judith St-Onge, DEC, Nassima Addour-Boudrahem, PhD, Gyan Prakash, MSc, Sung-Hoon Kim, PhD, Tristan Brunette-Clement, MD, Ghadd Alhajaj, MD, Lina Mougharbel, PhD, Elena Bruneau, BSc, Kenneth A. Myers, MD, PhD, Francois Dubeau, MD, Jason Karamchandani, MD, Jean-Pierre Farmer, MDCM, Jeffrey Atkinson, MD, Jeffrey Hall, MD, Chantal Chantal Poulin, MD, Bernard Rosenblatt, MDCM, Joel Lafond-Lapalme, MSc, Alexander Weil, MD, Catherine Fallet-Bianco, MD, Steffen Albrecht, MD,† Nahum Sonenberg, PhD, Jean-Baptiste Riviere, PhD, Roy W. Dudley, MD, MSc, PhD, and Myriam Srour, MDCM, PhD

Correspondence

Dr. Srour
myriam.srour@mcgill.ca

Neurol Genet 2023;9:e200103. doi:10.1212/NXG.000000000200103

Abstract

Background and Objectives

Somatic and germline pathogenic variants in genes of the mammalian target of rapamycin (mTOR) signaling pathway are a common mechanism underlying a subset of focal malformations of cortical development (FMCDs) referred to as mTORopathies, which include focal cortical dysplasia (FCD) type II, subtypes of polymicrogyria, and hemimegalencephaly. Our objective is to screen resected FMCD specimens with mTORopathy features on histology for causal somatic variants in mTOR pathway genes, describe novel pathogenic variants, and examine the variant distribution in relation to neuroimaging, histopathologic classification, and clinical outcomes.

Methods

We performed ultra-deep sequencing using a custom HaloPlex^{HS} Target Enrichment kit in DNA from 21 resected fresh-frozen histologically confirmed FCD type II, tuberous sclerosis complex, or hemimegalencephaly specimens. We mapped the variant alternative allele frequency (AAF) across the resected brain using targeted ultra-deep sequencing in multiple formalin-fixed paraffin-embedded tissue blocks. We also functionally validated 2 candidate somatic *MTOR* variants and performed targeted RNA sequencing to validate a splicing defect associated with a novel *DEPDC5* variant.

Results

We identified causal mTOR pathway gene variants in 66.7% (14/21) of patients, of which 13 were somatic with AAF ranging between 0.6% and 12.0%. Moreover, the AAF did not predict balloon cell presence. Favorable seizure outcomes were associated with genetically clear resection borders. Individuals in whom a causal somatic variant was undetected had excellent postsurgical outcomes. In addition, we demonstrate pathogenicity of the novel c.4373_4375dupATG and candidate c.7499T>A *MTOR* variants in vitro. We also identified a novel germline aberrant splice site variant in *DEPDC5* (c.2802-1G>C).

*These authors contributed equally to this work as cofirst authors.

†Retired since 2021.

From the Research Institute of the McGill University Health Centre (E.K., J.S.-O., N.A.-B., L.M., E.B., K.A.M., J.L.-L., J.-B.R., R.W.D., M.S.); Integrated Program in Neuroscience (E.K.), McGill University; Department of Specialized Medicine (A.A.), McGill University Health Centre; Department of Human Genetics (A.A., J.-B.R.), Faculty of Medicine; Goodman Cancer Centre (G.P., S.-H.K., N.S.), Department of Biochemistry, McGill University; Department of Pediatric Neurosurgery (T.B.-C., A.W.), Centre Hospitalier Universitaire Sainte-Justine, University of Montreal; Division of Pediatric Neurology (G.A., K.A.M., C.C.P., M.S.), Department of Pediatrics, McGill University, Montreal, Quebec, Canada; Department of Pediatrics (G.A.), Unaizah College of Medicine and Medical Sciences, Qassim University, Saudi Arabia; Department of Neurology and Neurosurgery (K.A.M., F.D., J.H., C.C.P., M.S.), McGill University Health Centre; Department of Pathology (J.K., S.A.), McGill University; Division of Neurosurgery (J.-P.F., J.A., R.W.D.), Department of Pediatric Surgery, McGill University Health Center; McGill University (B.R.); Department of Pathology (C.F.-B.), Centre Hospitalier Universitaire Sainte-Justine, University of Montreal, Quebec, Canada.

Go to Neurology.org/NG for full disclosures. Funding information is provided at the end of the article.

The Article Processing Charge was funded by authors.

This is an open access article distributed under the terms of the Creative Commons Attribution-NonCommercial-NoDerivatives License 4.0 (CC BY-NC-ND), which permits downloading and sharing the work provided it is properly cited. The work cannot be changed in any way or used commercially without permission from the journal.

Glossary

AAF = alternate allele frequency; CNV = copy number variant; EC = Engel classification; FCD = focal cortical dysplasia; FMCDs = focal malformations of cortical dysplasia; FFPE = formalin-fixed paraffin-embedded; HMEG = hemimegalencephaly; mTOR = mammalian target of rapamycin; PMG = polymicrogyria; TSC = tuberous sclerosis complex.

Discussion

The AAF of somatic pathogenic variants correlated with the topographic distribution, histopathology, and postsurgical outcomes. Moreover, cortical regions with absent histologic FCD features had negligible or undetectable pathogenic variant loads. By contrast, specimens with frank histologic abnormalities had detectable pathogenic variant loads, which raises important questions as to whether there is a tolerable variant threshold and whether surgical margins should be clean, as performed in tumor resections. In addition, we describe 2 novel pathogenic variants, expanding the mTORopathy genetic spectrum. Although most pathogenic somatic variants are located at mutation hotspots, screening the full-coding gene sequence remains necessary in a subset of patients.

Introduction

Focal malformations of cortical development (FMCDs) comprise a spectrum of developmental disorders ranging from focal cortical dysplasia (FCD) to hemimegalencephaly. The common denominator of these conditions is a disruption of the normal cytoarchitecture of the cerebral cortex, frequently resulting in medication-resistant epilepsy that usually requires surgical treatment. FCDs are classified into different neuropathologic subtypes (type Ia, Ib, Ic, IIa, IIb, IIIa, IIIb, IIIc, and IIId) based on the severity of cytoarchitectural disruption.¹ FCD type II is by far the most common in patients who undergo epilepsy surgery and is characterized on histology by loss of cortical lamination and large dysmorphic neurons without (type IIa) or with (type IIb) balloon cells.²

Recent studies have highlighted the role of hyperactivation of the mechanistic target of rapamycin (mTOR) pathway in a subset of FMCDs, which includes FCD type II, subtypes of polymicrogyria, and hemimegalencephaly.³⁻⁷ These disorders are now considered part of the same disease spectrum, termed “mTORopathies”, and share indistinguishable histopathologic features, namely disrupted cytoarchitecture and dysmorphic neurons with or without balloon cells. The mTOR pathway has an important role in cell growth, maturation, proliferation, and energy metabolism.⁸ Both somatic gain-of-function variants in activator genes (such as *MTOR*,⁹⁻¹² *AKT3*¹³, *RHEB*¹⁴, and *PIK3CA*¹⁵) and loss-of-function germline variants in negative regulator genes (such as *TSC1*, *TSC2*,¹⁶ *DEPDC5*,^{15,17-20} *PTEN*,^{21,22} *NPRL2*²³, and *NPRL3*^{23,24}) lead to upregulation of mTOR signaling, resulting in cellular overgrowth and abnormal migration.²⁵ Although pathogenic variants in a single allele of activator genes are sufficient to hyperactivate mTOR signaling, a two-hit allelic variant mechanism has been suggested for at least some negative regulator genes, such as *TSC1/2*^{16,26} and *DEPDC5*.^{19,26,27} More recent studies also suggest that there may be a synergistic second hit in another mTOR pathway

gene.²⁷⁻³¹ To date, the underlying cause of FMCDs is found in 15.6–63% of surgical samples, at alternate allele frequencies (AAFs) ranging from 0.14 to 33%.^{31,32}

This study aims to examine the sequence variant load of mTOR pathway pathogenic variants and their topographic distribution in relation to neuroimaging, histopathologic classification, and clinical outcomes; assess the diagnostic yield of screening mTOR pathway genes in FMCD specimens showing histologic features of mTORopathy; and characterize previously unreported mTOR pathway variants.

Methods

Patient Cohort and Specimens

As part of an ongoing epilepsy surgery biobanking program, we collect fresh-frozen and formalin-fixed and paraffin-embedded (FFPE) brain specimens and blood and/or saliva from patients undergoing epilepsy surgery at the Montreal Children’s Hospital, Montreal Neurologic Institute, and CHU Sainte-Justine Hospital. We collect between 1 to 7 fresh brain specimens per patient undergoing epilepsy surgery, which are snap-frozen on dry ice. For each of these specimens, the adjacent tissue is FFPE and analyzed by the neuropathology department. Additional FFPE blocks are also available for each patient. Neuropathologic diagnoses are performed according to the ILAE guidelines.³³

All patients who underwent epilepsy surgery between January 2016 and June 2019 in whom histopathology of the resected lesion confirmed an mTORopathy based on cortical dyslamination with dysmorphic neurons with or without balloon cells were included in this study. Presurgical evaluation and surgical procedures were performed as previously reported.³⁴ All patients underwent a 3T MRI. Clinical information, including age at seizure onset, seizure localization, developmental milestones, and postsurgical outcomes, was collected from medical records.

Standard Protocol Approvals, Registrations, and Patient Consents

This multicentric study had ethical approval from the research ethics committee of the McGill University Health Center (13-244-PED). All participants or their parents gave written informed consent.

Data Availability

All generated data are included in this article and associated Supplementary material. The raw data generated and/or analyzed during the study are available from the corresponding author on request.

Screening of mTOR Pathway Genes

For each patient, genomic DNA was extracted from fresh-frozen (Qiagen, QIAamp Fast DNA Tissue Kit), FFPE brain sections (Qiagen QIAamp DNA FFPE Tissue Kit) and peripheral blood or saliva (Qiagen, Puregene and DNA Genotek, PrepIt) using standard methods. We designed a custom panel of 13 genes (*AKT1*, *AKT2*, *AKT3*, *CCND2*, *DEPDC5*, *MTOR*, *NPRL2*, *NPRL3*, *PIK3CA*, *PIK3R2*, *PTEN*, *TSC1*, and *TSC2*) belonging to the mTOR pathway using a HaloPlex^{HS} Target Enrichment kit (Agilent Technologies). This capture method allows the identification of low allele frequency variants through the attachment of a unique barcode that permits the tracking of individual DNA molecules, thus avoiding enrichment bias and minimizing sequencing errors to allow a more accurate estimation of the level of mosaicism. Libraries were prepared according to the manufacturer's protocol from 50 ng of DNA extracted from the most histologically abnormal fresh-frozen brain specimen of each patient, except individual 12. Because brain tissue was unavailable in this individual, DNA was extracted from saliva and scraping of his hypertrophic tongue. Deep sequencing (approximately 1,500 reads) was performed on a MiSeq platform using paired end 150-bp reads. Sequenced reads were aligned to the human genome reference sequence (hg19) using BWA. A coverage of 99.2% of targeted bases was obtained by at least 100 reads in all samples. Variant calling was performed using a publicly available analytic pipeline (DnaSeq high Coverage Pipeline).³⁵ Candidate variants were retained if supported by at least 3 nonreference reads with a base quality threshold of 30 and an AAF of $\geq 0.5\%$. Heterozygous coding and splice site variants were retained if absent in gnomAD³⁶ and in-house controls. Variants were prioritized if previously reported in the literature or reported in COSMIC.³⁷ The pathogenicity of variants was determined based on the American College of Medical Genetics and Genomics (ACMG) Classification Guidelines.³⁸

Validation and Topographic Mapping of Pathogenic Variants

Candidate variants were confirmed by targeted ultra-deep sequencing (approximately 100,000-fold) in DNA extracted from fresh-frozen brain, blood, and/or saliva. In addition, we investigated the distribution of pathogenic variant loads across the resected brain by performing targeted sequencing

of DNA extracted from multiple FFPE brain tissue blocks (including those from previous surgeries). The region spanning the variant was amplified using custom intronic primers. Libraries were prepared using Nextera XT DNA Sample Preparation kit (Illumina) and sequenced on a MiSeq platform using paired end 150-bp reads. The variant was present in a specimen if it was found in $\geq 0.5\%$ of reads.

Functional Validation of Candidate mTOR Pathway Variants

To assess whether variants p.Asp1458dup and p.Ile2500Asn resulted in upregulation of the mTOR pathway, an in vitro transfection assay was used to probe for downstream hyperphosphorylation of P70-S6K1, a well-described marker for mTOR pathway hyperactivation.⁸ Candidate *MTOR* variants were cloned separately into a pcDNA3-Flag *MTOR* wild-type plasmids obtained from Addgene (Plasmid #26603), using QuikChange Lightning site-directed mutagenesis kit (Agilent). Mutant constructs were transiently cotransfected with P70-S6K1 in HEK293T cells to probe for hyperphosphorylation of P70-S6K1 at threonine 389. Four independent western blot repeats were performed. ImageJ analysis (Version 1.53j) was conducted for quantification of the signal intensity of the bands. Statistical tests applied were one-way analysis of variance (ANOVA), followed by the Dunnett post hoc test.

Investigation of Aberrant Splicing and Search for a Potential Second Hit in *DEPDC5*

Total RNA was extracted from the fresh-frozen brain of patient 14 and blood from the patient and her mother, and cDNA was synthesized according to standard protocols. To verify the aberrant splicing of *DEPDC5*, cDNA was amplified using a set of primers between exons 28 and exon 32 of *DEPDC5* (eFigure 1, links.lww.com/NXG/A637). We also amplified full-length *DEPDC5* mRNA by long-range PCR to look for a second pathogenic variant. The statistical framework mixture-of-isoforms (MISO) software was used to estimate the expression and effect of alternatively spliced exons and isoforms.³⁹ Finally, we searched for the presence of a somatic copy number variant (CNV) involving *DEPDC5* in the brain. DNA derived from patient 14 (fresh brain and blood) and her mother (blood) was genotyped using high-resolution SNP array CytoScan HD (Affymetrix, Santa Clara, CA) at the McGill Genome Innovation Center querying a total of 750,000 SNPs and 2.67 million CNV markers.

Genetic, Radiologic, and Clinical Correlations

We further delineated whether there was a relationship between pathogenic variant burden (AAF) and its topographic distribution, neuroimaging, histopathologic classification, clinical features, and postsurgical epilepsy outcomes. Chi-square, Fischer exact test, or *t* test was used to compare outcomes and clinical features between patient groups. Two-sided tests with *p*-values below 0.05 were considered statistically significant.

Results

Patients' Characteristics

A total of 47 individuals undergoing epilepsy were recruited between January 2016 and June 2019, and of them, 21 individuals had histologic mTORopathy features on resected brain (i.e., cortical dyslamination, dysmorphic neurons with or without balloon cells) and were included in this study. A summary of the clinical, radiologic, and histologic features and postsurgical seizure outcomes are described in Tables 1 and 2 and eTable 2 (links.lww.com/NXG/A640). Our cohort comprises 11 male and 10 female patients. The average age was 19.5 years (range: 2–60 years, median: 14 years), at seizure onset was 4.8 years (range: 1 day–20 years, median: 3 years) and at surgery was 15.5 years (range: 9 months–58 years, median: 11 years). All patients had drug-resistant focal epilepsy; 16 had FCD, 3 had HMEG (including one patient with congenital lipomatous overgrowth, vascular malformations, epidermal nevi, and scoliosis/skeletal/spinal (CLOVES) syndrome and 1 with hypomelanosis of Ito), one had polymicrogyria, and one had tuberous sclerosis complex (TSC). Fourteen individuals underwent a single surgery, and 7 had multiple surgeries. Histology was consistent with FCD type IIa in 14 individuals and FCD type IIb in 7 individuals. FMCD was located in a single lobe in 14 of the 21 (67%) individuals and involved the frontal lobe in 9 of 14 (64%), temporal lobe in 4 of 14 (29%), and cingulate cortex in 1 of 14 (7%). 3T brain MRI was considered normal in 7 individuals.

Diagnostic Yield of mTOR Gene Panel Screen

A total of 131 samples, including 37 fresh-frozen, 73 FFPE brain specimens, and 21 blood/saliva specimens, were collected from the 21 patients with histologic features of mTORopathy.

We identified disease-causing variants in 14 patients, representing a diagnostic yield of 66.7% (Table 1, Figure 1). Pathogenic variants were somatic in 13 patients and germline in one patient (Patient 14). Patient 14 carried a heterozygous germline splice site variant in *DEPDC5* (NM_001242896.1: c.2802-1G>C). Nine patients had somatic variants in *MTOR*, 2 in *PIK3CA*, one in *TSC2*, and one in *AKT3*. We detected variants with an AAF as low as 0.6%. Notably, 43% (9/21) of specimens screened with the Haloplex panel had an AAF of <5%. All variants were validated with targeted ultra-deep sequencing. In 11 patients, the somatic variants were previously reported and shown to result in hyperactivation of the mTOR pathway and thus deemed pathogenic. We were only able to detect the somatic pathogenic variant in blood or saliva/buccal swabs in 2 individuals, both of whom had evidence of extracerebral involvement: an individual with hemimegalencephaly as a manifestation of his CLOVES syndrome (individual 12) and one individual with a clinical diagnosis of TSC (individual 10 has hypomelanotic macules, facial angiofibromas, bilateral angiomyolipomas, subependymal nodules, and cortical/subcortical tubers; his previous clinical

testing on blood was negative, and we did not identify a second *TSC2* variant). Diagnostic yield was similar whether the FMCD was apparent on brain imaging (abnormal imaging in 10/14 with positive genetic yield vs 4/7 with negative genetic yield, $p = 0.64$).

Two Candidate *MTOR* Variants Result in mTOR Pathway Upregulation

We identified a novel somatic variant in *MTOR* (NM_004958.4), not previously associated with FCD: c.4373_4375dupATG (p.Asp1458dup). In addition, variant c.7499T>A (p.Ile2500Asn) was recently associated with FCD type II in a single patient and had not undergone functional studies.^{7,41} Both variants are absent in gnomAD and affect highly conserved residues. The c.4373_4375dupATG results in an in-frame single amino acid duplication of 55 amino acids upstream from the FAT domain, in close proximity to several other pathogenic variants (Figure 2). The p.Ile2500Asn substitution is located 31 amino acids before the FATC domain (Figure 2). A different amino acid substitution at the same position, p.Ile2500Phe, has been reported in 2 patients with FCD type II³¹ and 2 patients with hemimegalencephaly.^{7,41,45} Both p.Ile2500Asn and p.Ile2500Phe are linked in COSMIC to several samples of different carcinoma types (COSV63869065, COSM1730782, eTable 1, links.lww.com/NXG/A639) and associated with low-grade oncogenic renal tumors.⁴⁶ The c.4373_4375dupATG and c.7499T>A variants result in a 7-fold and 8-fold increase in P70-S6K1 phosphorylation ($p \leq 0.0001$ and $p \leq 0.001$), respectively, in vitro, demonstrating that they cause mTOR pathway upregulation (Figure 3).⁷

The c.7499T>A (p.Ile2500Asn) variant was detected at an AAF ranging between 1.2% and 7.6% (Figure 4A.c) in the brain specimen from patient 2, who developed focal seizures at age 16 months. Her initial 3T brain MRI was normal. Seizures were initially controlled with levetiracetam; however, the patient presented at 23 months of age in super-refractory status epilepticus, unresponsive to standard antiseizure medications and anesthetics.²⁴ An occipital brain biopsy revealed FCD type IIa. She subsequently underwent a right hemispherectomy, and histology revealed FCD type IIa features in all specimens examined. Similarly, the c.7499T>A variant was identified in all tested brain specimens (eTable 1, links.lww.com/NXG/A639). She died at age 24 months after 41 days of status epilepticus.

The c.4373_4375dupATG (p.Asp1458dup) variant was found at an AAF between 1.3% and 3.1% (Figure 4B.b) in brain specimens from patient 3, a 31-year-old woman with childhood-onset drug-resistant right frontal seizures. Her brain MRI was normal, and histology revealed FCD type IIa. She continues to have seizures despite 2 epilepsy surgeries.

Detection of Novel Germline Splice Site Variant in *DEPDC5*

We identified a novel germline variant affecting a canonical splice site (NM_001242896.1, c.2802-1G>C) of *DEPDC5* in

Table 1 Clinical Characteristics and Genetic Findings in Individuals With Identified Pathogenic mTOR Pathway Variants

Patient#	Current age (age Dcd), sex	Age at sz onset, last surgery	Clinical diagnosis	Development	3T brain MRI	Histology	Total # surgeries	Sz outcome ^a (f/u yrs)	Gene	Nucleotide, protein change	Novel vs prev. reported	Variant allele frequency		
												Brain ^b	Blood	Saliva
1	43 y, M	9 y/41 y	R hemisphere DRE, R HMEG and OVG	Learning disability	R HMEG	HMEG/FCD IIb	3	ECIV (2 y)	<i>MTOR</i>	c.4448G>A p.Cys1483Tyr	Prev. rep. ^{12,40}	8.5% [3.0–11.6%]	NA	Not detected
2	(2 y-Dcd), F	16 m/2 y	R hemisphere DRE	Normal	Normal*	FCD IIa	2	ECIV (Dcd)	<i>MTOR</i>	c.7499T>A, p.Ile2500Asn	Prev. rep. ⁴¹	3.5% [1.2–7.6%]	Not detected	NA
3	32 y, F	12 y/29 y	R posterior cingulate DRE	Learning disability	Normal	FCD IIa	2	ECIV (2 y)	<i>MTOR</i>	c.4373_4375dupATG, p.Asp1458dup	Novel	3.1% [1.3–3.1%]	Not detected	Not detected
4	21 y, M	3 y/15 y	R frontal lobe DRE	Normal	R frontoparietal FCD, R subcortical parieto-occipital cysts	FCD IIb	3	ECII (6 y)	<i>MTOR</i>	c.4447T>C p.Cys1483Arg	Prev. rep. ¹²	2.6% [0.6–8.8%*]	Not detected	Not detected
5	8 y, M	18 m/5 y	R lobe focal DRE	Normal	R frontal FCD	FCD IIb	1	ECII (1.25 y)	<i>MTOR</i>	c.6644C>A, p.Ser2215Tyr	Prev. rep. ⁴²	0.9% [0.9–1.9%*]	Not detected	NA
6	8 y, F	2 m/5 y	Focal left temporal DRE	Normal	Normal	FCD IIa	3	ECIV (1.8 y)	<i>MTOR</i>	c.6644C>T, p.Ser2215Phe	Prev. rep. ⁴²	0.9% [2.1–5.4%*]	NA	NA
7	9 y, M	3 y, 3 y	Left frontal DRE	Normal	L frontal FCD	FCD IIb	1	ECI (6 y)	<i>MTOR</i>	c.5930C>A p.Thr1977Lys	Prev. rep. ¹²	0.8% [0.8–3.5%*]	Not detected	NA
8	45 y, F	9 y, 42 y	R frontal DRE	Normal	Normal	FCD IIa	1	ECI (1 y)	<i>MTOR</i>	c.6644C>T, p.Ser2215Phe	Prev. rep. ⁴²	0.7% [0.7%*]	Not detected	NA
9	14 y, F	7 y, 10 y	L parietotemporal DRE	Normal	L supramarginal gyrus FCD	FCD IIb	1	ECI (1.5 y)	<i>MTOR</i>	c.5930C>A, p.Thr1977Lys	Prev. rep. ¹²	0.6% [0.6%*]	Not detected	NA
10	5 y, M	3 m, 4 y	TSC, left hemispheric DRE	GDD, ID	Multiple R>L tubers and subependymal nodules	FCD IIb	2	ECIII (3.75 y)	<i>TSC2</i>	c.2356-1G>A, p.?	Novel	9.4% [6.3–9.4%]	6.3%	3.6%
11	8 y, M	1 d, 9 m	L hemispheric DRE, L HMEG	GDD, ID	L HMEG	HMEG/FCD IIa	1	ECIV (3.92 y)	<i>AKT3</i>	c.49G>A, p.Glu17Lys	Prev. rep. ³¹	4.9% [1.3–11.0%]	NA	Not detected
12	19 y, M	1 d, 1 y	CLOVES syndrome, R HMEG	Severe ID, ASD	R HMEG	HMEG/FCD IIa	1	ECI (na)	<i>PIK3CA</i>	c.1624G>A, p.Glu542Lys	Prev. rep. ³²	NA	Not detected	4.85–10.32% ^c
13	14 y, M	6 y, 7 y	Right frontal DRE	GDD	R frontal PMG	PMG/FCD IIa	x	ECII (6 y)	<i>PIK3CA</i>	c.1624G>A, p.Glu542Lys	Prev. rep. ³²	12.0% [5.1–22.7%]	NA	NA
14	19 y, F	1d, 13 y	Right frontal lobe DRE ^d	Severe ID	R frontal FCD	FCD IIa	3	ECIII (3 y)	<i>DEPDC5</i>	c.2802-1G>C	Novel	33.0% [33.0–59.8%]	50.8%	NA

Abbreviations: ASD = autism spectrum disorder; CLOVES = congenital lipomatous overgrowth, vascular malformations, epidermal nevi, and scoliosis/skeletal/spinal syndrome; d = day; Dcd = deceased; DRE = drug-resistant epilepsy; f/u = follow-up; F = female; FCD = focal cortical dysplasia; GDD = global developmental delay; HMEG = hemimegalencephaly; ID = intellectual disability; L = left; M = male; m = months; NA = not available; OVG = overgrowth; PMG = polymicrogyria; Prev. rep. = previously reported; R = right; sz = seizure; TSC = tuberous sclerosis complex; y = years.

^a Seizure outcome according to Engel classification (Engel 1993).

^b Variant allele frequency obtained from DNA extracted from fresh-frozen resected brain tissue. The range of allele frequencies across all samples tested are provided in brackets. * indicates that the pathogenic variant is undetectable in some specimens.

^c Buccal swab of hemihypertrophic tongue.

^d This patient also harbors a likely pathogenic heterozygous variant in *EBF3* (c.431A>G, p.Gln144Arg) that likely underlies her severe ID and facial dysmorphism. The Engel Epilepsy Surgery Outcome Scale was used to classify postsurgical outcomes (Engel Class I: freedom from disabling seizures; Class II: rare disabling seizures (almost seizure free); Class III: worthwhile seizure reduction; Class IV: no worthwhile improvement).^{43,44}

Table 2 Clinical Characteristics of FCD Individuals With Negative mTOR Pathway Genetic Screening

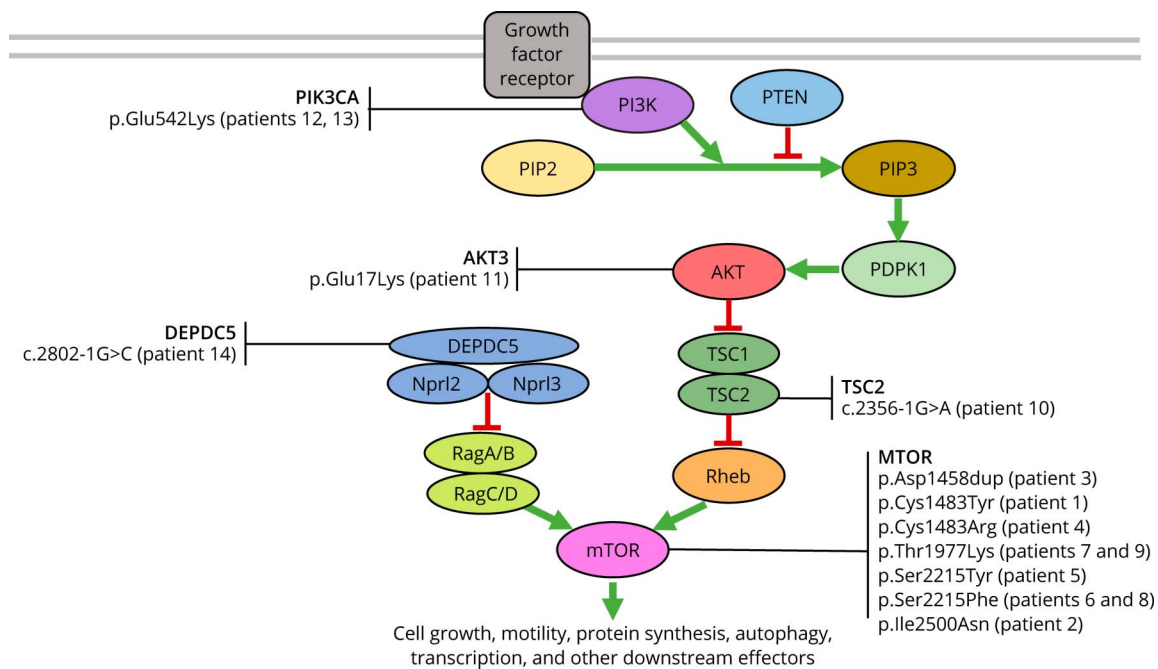
Patient #	Current age, sex	Age at sz onset, at last surgery	Clinical diagnosis (duration of epilepsy)	Development	3T brain MRI	Histology	Total number of surgeries	Sz outcome (f/u)
15	20 y, F	8 y, 14	Right frontal DRE (6 y)	Normal	R frontal FCD	FCD type IIa	1	ECl (6 y)
16	11 y, M	3 y, 7 y	Left Fronto-central-parietal DRE epilepsy (4 y)	Normal	Normal	FCD type IIa	1	ECl (2 mo)
17	14 y, F	2 y, 11 y	Left SMA DRE (9 y)	Normal	Normal	FCD type IIa	2	ECl (4 y)
18	14 y, F	10 y, 11 y	Right SMA DRE (1 y)	Normal language disorder	Normal	FCD type IIa	1	ECl (3 y)
19	11 y, F	4 y, 4 y	Left temporal DRE (4 m)	Normal	Left parieto-temporal FCD	FCD type IIb	1	ECl (7 y)
20	60 y, M	20 y, 58 y	Left temporal DRE (38 y)	Normal	Left hippocampal sclerosis	FCD type IIa	1	ECl (2 y)
21	32 y, M	10 m	Left temporal DRE (28 y)	Normal	Left hippocampal FLAIR signal abnormality	FCD type IIa	1	ECl (3 y)

Abbreviations: DRE = drug-resistant epilepsy; FCD = focal cortical dysplasia; ECl = Engel class I; f/u = follow-up; m = months; SMA = supplementary motor area; sz = seizure; y = year.

patient 14, inherited from her asymptomatic mother. This variant has not been previously reported, is absent in control databases (gnomAD), and is classified as pathogenic based on ACMG Guidelines. Targeted sequencing of *DEPDC5* cDNA derived from the patient's blood and brain revealed that the

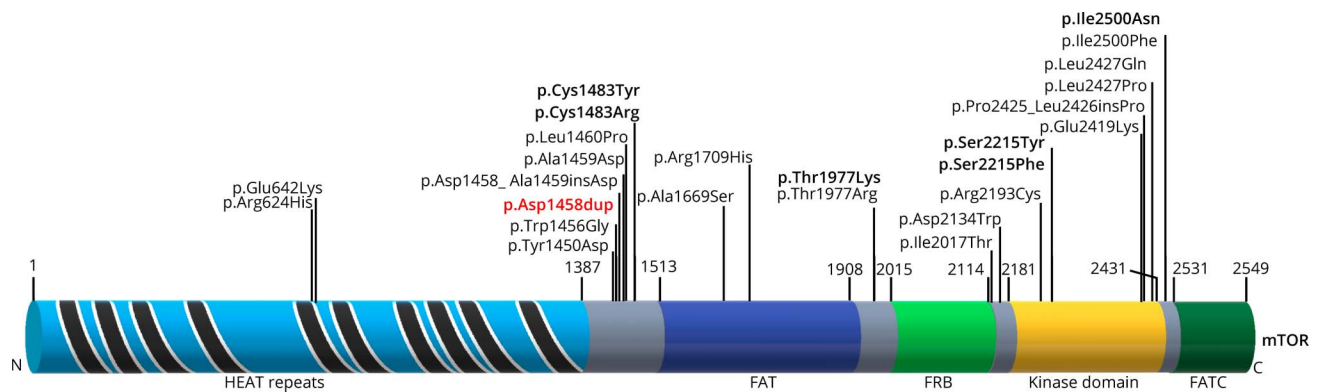
c.2802-1G>C variant results in aberrant splicing and retention of intron 29 (eFigure 1A, links.lww.com/NXG/A637) predicted to shift the reading frame. Moreover, the probabilistic model of RNA-seq obtained with MISO and displayed with Sashimi revealed the presence of extra read densities between

Figure 1 Pathogenic Variants in mTOR Pathway Genes Identified in Our FMCD Cohort



Representation of 14 variants detected with their corresponding patient number and location. Variants in *MTOR*, *PIK3CA*, and *AKT3* are somatic gain-of-function variants in positive regulators of the mTOR pathway. *DEPDC5* and *TSC2* are loss-of-function variants in negative regulators of the mTOR pathway. FMCD = focal malformations of cortical development; mTOR = mammalian target of rapamycin.

Figure 2 Distribution of MTOR Pathogenic Variants Associated With FMCDs



Previously reported (in black) and novel (in red) pathogenic variants associated with FMCDs are indicated. Bolded substitutions were also found in our cohort. The mTOR protein contains 20 tandem HEAT repeats that provide protein-protein interactions with the mTOR regulatory proteins Raptor and Rictor, the FAT modulatory domain, the FKBP12-rapamycin binding domain (FRB), the Ser/Thr kinase domain, and the FATC modulatory domain. There is a clustering of variants between the HEAT repeats and FAT domain, as well as within and close to the kinase domain. FMCDs = focal malformations of cortical development; mTOR = mammalian target of rapamycin.

exon 29 and 30, demonstrating intron 29 retention (eFigure 1B). We searched for a somatic variant or CNV involving *DEPDC5*; however, a second hit was not identified after sequencing of full-length *DEPDC5* cDNA and whole-genome SNP array.

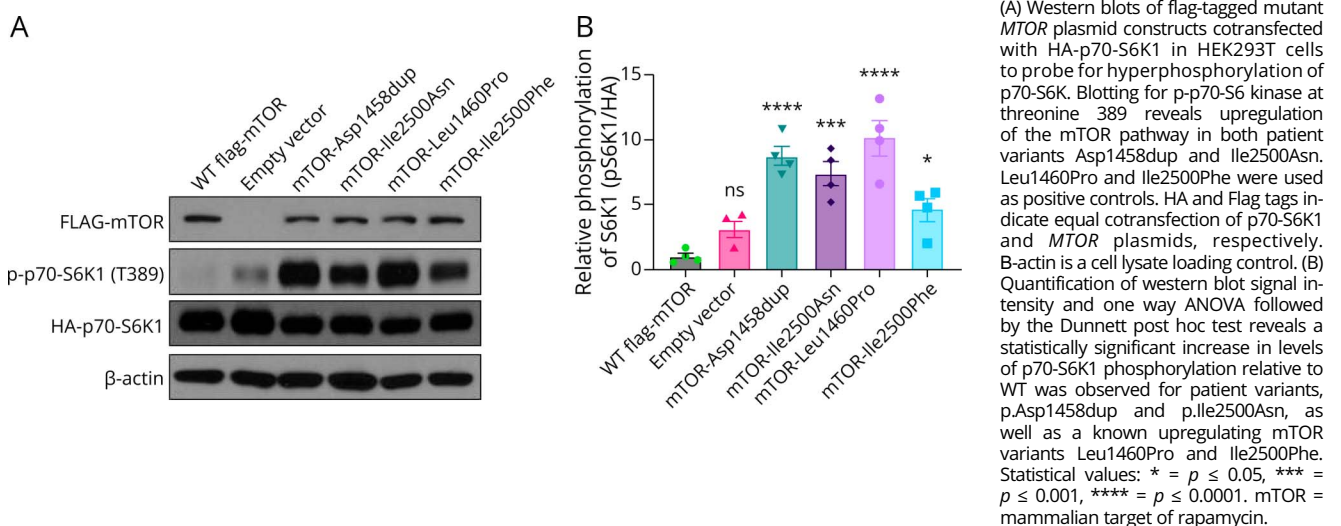
Variant Load, Topographic Distribution, Histology, and Clinical Outcomes

For the 14 individuals in whom we identified a causal somatic mTOR pathway variant, we further studied a total of 103 brain specimens, including 73 FFPE specimens, to assess the AAF and distribution of the variants across multiple brain regions (average of 7.35 brain specimens per patient). A summary of the topographic distribution of the variants for each patient is depicted in eFigure 2 (links.lww.com/NXG/A638).

All solved FCDs in our cohort had somatic pathogenic *MTOR* variants. Pathogenic somatic variants were found in *AKT3* and *PIK3CA* in larger cerebral lesions, namely hemimegalencephaly and polymicrogyria.

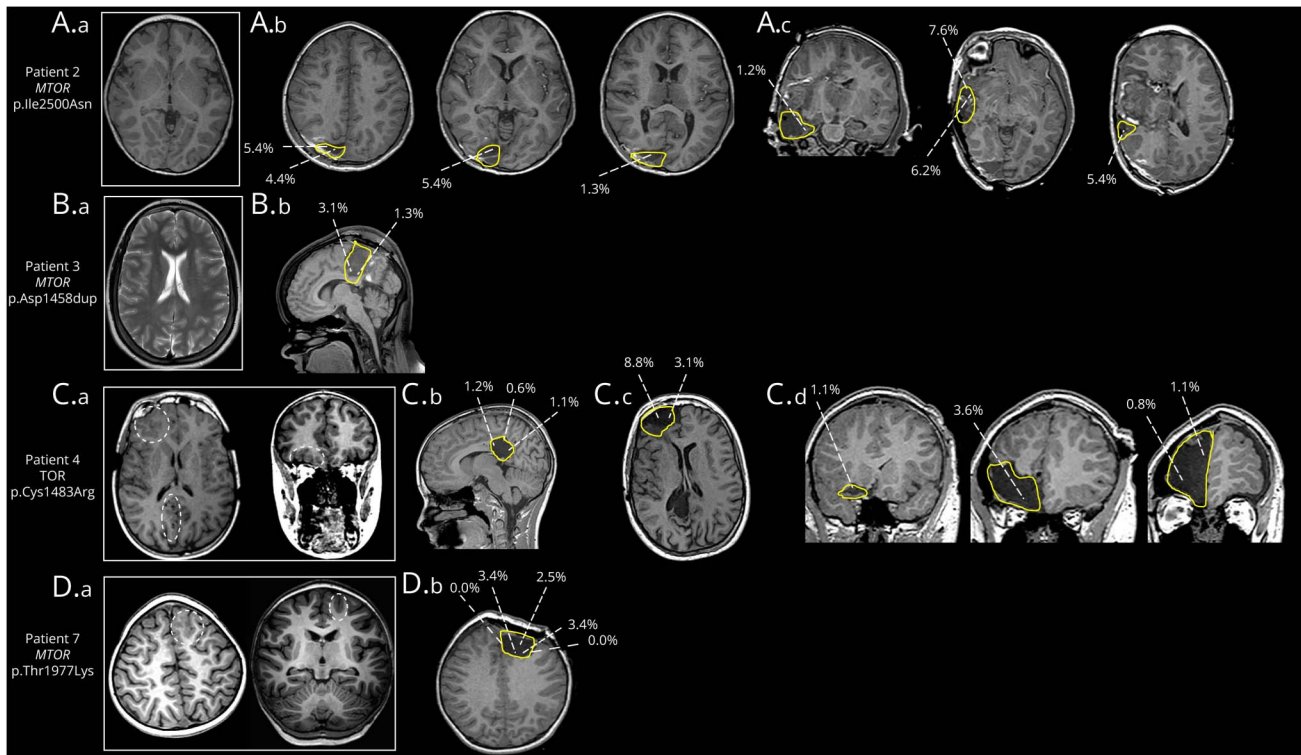
In general, the load and topographic distribution of the somatic pathogenic variants correlated with the size of the FMCD on MRI and based on the distribution of histopathologic abnormalities: more extensive lesions were associated with higher maximal AAFs (eFigure 2, links.lww.com/NXG/A638 and eTable 2, links.lww.com/NXG/A640). For example, patients with hemimegalencephaly (individuals 1, 11, and 12) and extensive polymicrogyria (individual 13) had the highest maximal AAF (maximum AAF ranges 10.3%–22.7%). By contrast,

Figure 3 Functional Validation of Candidate MTOR Variants



(A) Western blots of flag-tagged mutant *MTOR* plasmid constructs cotransfected with HA-p70-S6K1 in HEK293T cells to probe for hyperphosphorylation of p70-S6K. Blotting for p-p70-S6 kinase at threonine 389 reveals upregulation of the mTOR pathway in both patient variants Asp1458dup and Ile2500Asn. Leu1460Pro and Ile2500Phe were used as positive controls. HA and Flag tags indicate equal cotransfection of p70-S6K1 and *MTOR* plasmids, respectively. B-actin is a cell lysate loading control. (B) Quantification of western blot signal intensity and one way ANOVA followed by the Dunnett post hoc test reveals a statistically significant increase in levels of p70-S6K1 phosphorylation relative to WT was observed for patient variants, p.Asp1458dup and p.Ile2500Asn, as well as a known upregulating mTOR variants Leu1460Pro and Ile2500Phe. Statistical values: * = $p \leq 0.05$, *** = $p \leq 0.001$, **** = $p \leq 0.0001$. mTOR = mammalian target of rapamycin.

Figure 4 Examples of Mapping Somatic Variants and Their AAF Across Resected Brain



Preoperative (boxed) and postoperative brain MRIs of patients 2 (A), 3 (B), 4 (C), and 4 (D). Yellow lines indicate the outline of the resected brain. The AAF frequency of the somatic pathogenic variants was obtained from targeted sequencing of DNA extracted from FFPE specimens corresponding to the indicated regions. Preoperative MRIs were reported as normal in patients 2 (A) and 3 (B). Patient 4 had right parieto-occipital cystic lesions and an extensive FCD in the right orbitofrontal lobe (dotted white circles, C), and patient 7 (D) had a right frontal bottom of sulcus FCD (dotted white circles, D). AAF = alternative allele frequency; FCD = focal cortical dysplasia; FFPE = formalin-fixed paraffin-embedded.

patients with FCD had a lower maximum pathogenic variant load (maximum AAF range for FCD 0.6–8.88% and average maximum AAF 3.74% in FCD vs 15.1% in PMG/HMG, $p = 0.0053$); even within the FCD subgroup, those with histopathologic extensive lesions (patients 2 and 4) had higher maximal AAF.

In general, somatic pathogenic variants were detected in tissue specimens displaying histologic abnormalities (eTable 2, links.lww.com/NXG/A640). We always identified the somatic pathogenic variants in specimens that were frankly histologically abnormal and consistent with FCD type II. Moreover, almost all histologically normal specimens showed the absence of a causal variant. However, it is important to note that there were rare specimens considered histologically normal in which we identified the presence of the somatic pathogenic variant at low levels. For example, in patient 4, we detected the somatic pathogenic variant at an AAF of 0.6 and 1.2% in DNA extracted from FFPE blocks from the right occipital lobe that were considered normal; in this patient, the epicenter of the FCD and the epileptogenic zone was much more anterior in the right frontal lobe where the histology was frankly abnormal, and the AAF was up to 8.8%.

We did not find a significant correlation between maximum variant load and histologic diagnosis of FCD type IIa vs IIb in

our samples (average maximum AAF 8.4% in FCD2a vs 6.0% in 2b, $p = 0.5227$). Patients with somatic *MTOR* pathogenic variants with similar AAF ranges could have either FCD type IIa or IIb on histology. Furthermore, when comparing the AAF and histologic findings across multiple brain specimens from the same patient, there was no relationship between AAF and the presence of balloon cells. For example, in patient 1 with the hemimegalencephaly/*MTOR* variant, balloon cells were identified in only one of the 13 FFPE specimens with a variant load of 3.9%; all other specimens showed the presence of dysmorphic neurons without balloon cells, with variant loads ranging between 3.3 and 11.6%. Similarly, in patient 4 with the *MTOR* variant, FFPE specimens with balloon cells had an AAF at 1.1%–3.3%, and the specimen with the highest AAF at 8.8% displayed no balloon cells.

Individuals with *PIK3CA* and *AKT3* variants were more likely to have neonatal-onset seizures than the remainder of the cohort (2/3 vs 0/18, $p = 0.0143$). There was also a correlation between neurodevelopmental outcome and causal gene: All individuals with somatic *MTOR* variants had normal development and intelligence, whereas those with *AKT3* or *PIK3CA* variants had global developmental delay and intellectual disability (GDD/IDD in 0/9 vs 4/4, $p = 0.0014$).

Patients with good surgical outcomes tended to have lower pathogenic variant loads and surgical margins with normal histology without the causal variant (Table 1). It is interesting to note that all 7 individuals from our cohort in whom we were unable to identify the underlying genetic etiology were seizure-free postresection, with Engel classification I (Table 2) (ECI-II in 7/13 with somatic variants identified vs 7/7 with no somatic variant identified, $p = 0.0515$). These patients also had histologically normal surgical margins.

Discussion

In this study, we genetically characterized a total of 131 specimens (including fresh-frozen and FFPE brain specimens, blood, and saliva) from 21 patients with FMCD with histologic features of mTORopathy.

We demonstrate that systematic screening of abnormal cerebral specimens using an mTOR pathway gene panel has a high diagnostic yield of 66.7%. This yield is high compared with the range previously reported in the literature (15.6%–63%).^{31,32} A further breakdown of the diagnostic yield shows that mTOR pathway variants underlie 86% (6/7) of FCD type IIb patients but only 53% (8/15) of FCD type IIa patients. Several factors may account for this high yield: We had access to fresh affected specimens of small size, which gave us a high resolution of the variations within the pathologic tissue and allowed for the enhanced detection of somatic variants at lower AAF; we chose the most abnormal specimens based on the histology of the adjacent tissue sections, and finally, we screened the full coding regions of the genes.

We confirmed many of the previously published observations, although our cohort included a modest number of patients. As noted by Baldassari et al. (2019)³⁰ and Pirozzi et al. (2022),^{31,47} we found that the highest AAFs were usually, although not strictly, associated with more extensive cortical lesions and that *PIK3CA* and *AKT3* were associated with large lesions such as hemimegalencephaly or polymicrogyria. Similarly, AAF appeared to correlate with histologic findings: cortical regions with absent histologic FCD features had negligible or undetectable pathogenic variant loads, whereas specimens with frank histologic abnormalities had detectable pathogenic variants. Our findings support the conclusions by Lee et al. (2023) and Baldassari et al. that the density of the dysmorphic cells correlated with the AAF.^{31,48} Of note, we did not observe any clear correlation between the histologic subtype of FCD type II (i.e., IIa or IIb) and AAF because regions of similar variant load may demonstrate the presence or absence of balloon cells; studies including a larger number of specimens will be required to confirm this observation.

The findings from our cohort support the previously noted correlation between *PIK3CA* or *AKT3* variants and poor neurodevelopmental outcome³¹ because all our patients with *PIK3CA* or *AKT3* variants have global developmental

delay/intellectual disability, whereas development was normal in all patients with *MTOR* variants. Note that poor neurodevelopmental outcome does not seem to be related only to the lesion size because patient 1 with the hemimegalencephaly and *MTOR* variant had normal development and intelligence, suggesting that poor cognitive outcome is not only associated with the topographic extent of the cortical malformation. Our cohort also supports neonatal onset of seizures with *PIK3CA* or *AKT3* compared with *MTOR*.

Of interest all patients with no identified pathogenic variant had good postsurgical epilepsy outcomes (Engel Class I, see Table 2). A possible explanation for this is that the AAF of the pathogenic variant was below our method's detection threshold and that the DNA was extracted from sections that were not pathologic and did not contain mutant cells, implying that a smaller FCD or one with a low pathogenic variant AAF is associated with better postsurgical outcome. Other potential reasons for not identifying the causal pathogenic variant include the presence of a pathogenic variant outside of the coding regions, deletions, structural rearrangements, and genes absent from our panel.⁴⁷

As illustrated in our study, the variable levels of pathogenic variants across FCDs raise important questions as to whether there is a tolerable variant level and whether the surgical margins of the resected FCD should be clean, as performed in tumor resections. The relationship between variant load, epileptogenic zone, and focus are still unknown, and larger-scale studies with combined intracranial recording, genetic, and histopathologic analysis and long-term seizure outcome are needed to address this matter.

We describe 2 novel somatic pathogenic variants responsible for FMCDs and illustrate that, although most pathogenic variants are recurrent, they may be present outside of mutation hotspots. Therefore, screening only for recurrent mutations is insufficient to identify causal pathogenic variants in patients with mTORopathies.

We performed functional validation of 2 variants in *MTOR*, p.Ile2500Asn and p.Asp1458dup, in patients with FCD type IIa and demonstrated using an in vitro assay that these variants result in hyperphosphorylation of P70-S6K1, indicating they are pathogenic and cause mTOR pathway upregulation. We also report a novel germline canonical splice site variant in *DEPDC5* (c.2802-1G > C) and show that it results in aberrant splicing leading to a frameshift. *DEPDC5* encodes for DEP domain containing 5, a member of the GATOR1 complex (GAP activity toward Rags complex 1) and, along with *NPRL2* and *NPRL3*, acts as a negative regulator of mTORC1.²⁶ Variants in *DEPDC5* are typically loss of function, with only a few recurrent variants reported. It has been hypothesized that a second-hit mechanism may be required to generate FCDs, as previously observed in cancer⁴⁸ and TSC.^{15,25} To date, this phenomenon has been demonstrated 6 times in GATOR1 genes for FCD.^{17,22,23,27,29-31} We did not

identify an additional pathogenic somatic variant in our patient.

Many of the somatic variants identified in our cohort were recurrent and involved substitution of the same amino acid. In *MTOR*, 2 patients had substitutions at p.Cys1483, 2 at p.Thr1977, and 3 at p.Ser2215. The p.Cys1483 amino acid is located 30 amino acids upstream of the FAT catalytic domain, where the N-terminal portion of the domain is required for binding of the regulator proteins Raptor and Rictor.⁴⁹ The p.Thr1977 variant is located 38 amino acids upstream of the rapamycin binding FRB domain and is thought to act as a gatekeeper at mTOR's catalytic cleft.⁴⁹ The p.Ser2215 variant is located just outside the $\alpha 3$ helix domain at the active site of the mTOR kinase, and its substitution has been previously demonstrated to upregulate mTOR through a gain-of-function sequence variant mechanism^{11,12,19,31,42} (Figure 2). Similarly, 2 patients had the identical p.Glu542Lys substitution in *PIK3CA*, which has previously been observed in hemimegalencephaly⁵⁰ and is frequently observed in tumors (COSV55873227 in COSMIC). This substitution disrupts an inhibitory charge-charge interaction with the p85 α regulatory subunit by affecting the catalytic region of the PI3K helical domain.⁴⁷

A few limitations of our study need to be mentioned. First, our study included a relatively small number of patients, which limits our ability to find statistically significant differences between groups and may also increase our margin of error. Nevertheless, our findings were in keeping with previous studies. Second, potential disease-causing variants may be present below the minimal AAF detection threshold (i.e., <0.005) for Haloplex^{HS} or lie in promoter regions or introns not covered by our panel. Third, *RHEB* (MIM* 601293)¹⁴ and *RPS6* (MIM* 180460),²⁸ which have recently been shown to be implicated in FCD pathogenesis, were not included in our gene panel. Fourth, we have investigated somatic CNV only in the individual harboring the *DEPDC5* variant but not in other patients.⁵¹ Finally, determination of the mosaic gradient of the somatic variants was performed on DNA extracted from FFPE and not fresh-frozen tissue as we did not have access to many fresh-frozen specimens per patient; although there is concern that fixing introduces DNA artifacts and may affect variant calling, it has been shown that sequencing of somatic variants in FFPE tissue is highly concordant with results from fresh tissue.⁵²

In summary, through the study of 103 specimens, we provide a compelling demonstration of the mosaic pattern of the somatic pathogenic variants in mTORopathies and show an association between the level of mosaicism, histopathologic findings, and clinical outcomes, concordant with previous studies. Cortical regions without histologic FCD features had negligible or undetectable pathogenic variant loads, whereas specimens with frank histologic abnormalities had detectable pathogenic variants. Seizure outcomes were favorable when resection borders were genetically clear, and individuals without an identified causal somatic variant had excellent postsurgical outcomes after

surgery. In addition, our study demonstrates that screening fresh-frozen specimens using a custom HaloPlexHs mTOR pathway gene panel results in a high diagnostic yield. We identify a novel somatic *MTOR* variant and provide in vitro evidence of pathogenicity, highlighting the importance of screening the full coding regions in mTORopathy lesions. We also describe a novel germline *DEPDC5* splice site mutation and show its impact on mRNA splicing. Routine molecular testing and integration of genetic results into the classification and diagnosis of FMCDs will be key to enhancing the characterization of FMCD cohorts, improving our understanding of underlying pathophysiology and allowing development of novel targeted treatment options and personalized medicine.⁵³

Acknowledgment

The authors thank the patients and families for participating in this study. E. Krochmalnek's graduate training was supported by the FRQS, McGill University's Faculty of Medicine Neurology and Neurosurgery Excellence Award, and MUHC Desjardins Studentship Award. Accogli's fellowship training was supported by the Mel Hoppenheim Fund (Montreal Children's Foundation) and the Rotary Foundation. The authors thank the Agilent team for their support in SureCall analysis. M. Srouf holds a Fonds de Recherche de Santé Quebec salary award.

Study Funding

This manuscript has been funded by Fondation Pierre Lavoie, CIHR/Sick Kids New Investigator Operating Award (NI16-028), Montreal Children's Hospital Foundation (Husain Family Endowment).

Disclosure

The authors report no relevant disclosures. Go to Neurology.org/NG for full disclosures.

Publication History

Received by *Neurology: Genetics* April 21, 2023. Accepted in final form September 6, 2023. Submitted and externally peer reviewed. The handling editor was Editor Stefan M. Pulst, MD, Dr med, FAAN.

Appendix Authors

Name	Location	Contribution
Eric Krochmalnek, MSc	Research Institute of the McGill University Health Centre; Integrated Program in Neuroscience, McGill University, Montreal, Quebec, Canada	Drafting first version of manuscript/revision of the manuscript for content, major role in the acquisition of data and analysis or interpretation of data
Andrea Accogli, MD	Department of Specialized Medicine, Division of Medical Genetics, McGill University Health Centre; Department of Human Genetics, Faculty of Medicine, McGill University, Montreal, Quebec, Canada.	Drafting first version of manuscript/revision of the manuscript for content, major role in the acquisition of data and analysis or interpretation of data

Appendix (continued)

Name	Location	Contribution
Judith St-Onge, DEC	Research Institute of the McGill University Health Centre, Montreal, Quebec, Canada	Revision of the manuscript, major role in experimentation and acquisition of data
Nassima Addour-Boudrahem, PhD	Research Institute of the McGill University Health Centre, Montreal, Quebec, Canada	Drafting/revision of the manuscript/acquisition and interpretation of data/recruitment of patients/administrative support
Gyan Prakash, MSc	Goodman Cancer Centre, Department of Biochemistry, McGill University, Montreal, Quebec, Canada	Revision of the manuscript, role in experimentation and acquisition of data
Sung-Hoon Kim, PhD	Goodman Cancer Centre, Department of Biochemistry, McGill University, Montreal, Quebec, Canada	Revision of the manuscript, role in experimentation and acquisition of data
Tristan Brunette-Clement, MD	Department of Pediatric Neurosurgery, Centre Hospitalier Universitaire Sainte-Justine, University of Montreal, Montreal, Quebec, Canada	Revision of the manuscript, acquisition of data
Ghadd Alhajaj, MD	Division of Pediatric Neurology, Department of Pediatrics, McGill University, Montreal, Quebec, Canada; Department of Pediatrics, Unaizah College of Medicine and Medical Sciences, Qassim University, Qassim, Saudi Arabia	Revision of the manuscript, acquisition of data
Lina Mougharbel, PhD	Research Institute of the McGill University Health Centre, Montreal, Quebec, Canada	Revision of the manuscript, role in experimentation, acquisition and analysis of data
Elena Bruneau, BSc	Research Institute of the McGill University Health Centre, Montreal, Quebec, Canada	Revision of the manuscript, role in experimentation
Kenneth A. Myers, MD, PhD, CCSN	Research Institute of the McGill University Health Centre; Division of Pediatric Neurology, Department of Pediatrics, McGill University; Department of Neurology and Neurosurgery, McGill University Health Centre, Montreal, Quebec, Canada	Revision of the manuscript, contribution of patients and clinical data
François Dubeau, MD	Department of Neurology and Neurosurgery, McGill University Health Centre, Montreal, Quebec, Canada	Revision of the manuscript, contribution of patients and clinical data
Jason Karamchandani, MD	Department of Pathology, McGill University, Montreal, Quebec, Canada	Revision of the manuscript, contribution of clinical data

Appendix (continued)

Name	Location	Contribution
Jean-Pierre Farmer, MDCM, FRCS	Division of Neurosurgery, Department of Pediatric Surgery, McGill University Health Center, Montreal, Quebec, Canada	Revision of the manuscript, collection of specimens, contribution of patients and clinical data
Jeffrey Atkinson, MD	Division of Neurosurgery, Department of Pediatric Surgery, McGill University Health Center, Montreal, Quebec, Canada	Revision of the manuscript, collection of specimens, contribution of patients and clinical data
Jeffery Hall, MD FRCS	Department of Neurology and Neurosurgery, McGill University Health Centre, Montreal, Quebec, Canada	Revision of the manuscript, collection of specimens, contribution of patients and clinical data
Chantal Poulin, MD	Division of Pediatric Neurology, Department of Pediatrics, McGill University; Department of Neurology and Neurosurgery, McGill University Health Centre, Montreal, Quebec, Canada	Revision of the manuscript, contribution of patients and clinical data
Bernard Rosenblatt, MDCM	Division of Pediatric Neurology, Department of Pediatrics, McGill University; Department of Neurology and Neurosurgery, McGill University Health Centre, Montreal, Quebec, Canada	Revision of the manuscript, contribution of patients and clinical data
Joël Lafond Lapalme, MSc	Research Institute of the McGill University Health Centre, Montreal, Quebec, Canada	Revision of the manuscript, bioinformatic analysis of data
Alexander G. Weil, MD	Department of Pediatric Neurosurgery, Centre Hospitalier Universitaire Sainte-Justine, University of Montreal, Montreal, Quebec, Canada	Revision of the manuscript, collection of specimens, contribution of patients and clinical data
Catherine Fallet-Bianco, MD	Department of Pathology, Centre Hospitalier Universitaire Sainte-Justine, University of Montreal, Montreal, Quebec, Canada	Revision of the manuscript, collection, analysis and interpretation of data
Steffen Albrecht, MD	Department of Pathology, McGill University, Montreal, Quebec, Canada	Revision of the manuscript, collection, analysis and interpretation of data
Nahum Sonenberg, PhD	Goodman Cancer Centre, Department of Biochemistry, McGill University, Montreal, Quebec, Canada	Revision of the manuscript, analysis and interpretation of data, supervision
Jean-Baptiste Riviere, PhD	Research Institute of the McGill University Health Centre, Montreal, Quebec, Canada	Revision of the manuscript, bioinformatic analysis of data

Continued

Appendix (continued)

Name	Location	Contribution
Roy W. Dudley, MD, MSc, PhD	Research Institute of the McGill University Health Centre; Division of Neurosurgery, Department of Pediatric Surgery, McGill University Health Center, Montreal, Quebec, Canada	Revision of the manuscript, collection of specimens, analysis and interpretation of data
Myriam Srour, MDCM, PhD	Research Institute of the McGill University Health Centre; Division of Pediatric Neurology, Department of Pediatrics, McGill University; Department of Neurology and Neurosurgery, McGill University Health Centre, Montreal, Quebec, Canada	Conception and design of the study, supervision, drafting and revision of the manuscript; analysis and interpretation of data

References

- Blumcke I, Spreafico R. An international consensus classification for focal cortical dysplasias. *Lancet Neurol*. 2011;10(1):26-27. doi:10.1016/S1474-4422(10)70225-8
- Blumcke I, Spreafico R, Haaker G, et al. Histopathological findings in brain tissue obtained during epilepsy surgery. *N Engl J Med*. 2017;377(17):1648-1656. doi:10.1056/NEJMoa1703784
- Baybis M, Yu J, Lee A, et al. mTOR cascade activation distinguishes tubers from focal cortical dysplasia. *Ann Neurol*. 2004;56(4):478-487. doi:10.1002/ana.20211
- Crino PB. mTOR: a pathogenic signaling pathway in developmental brain malformations. *Trends Mol Med*. 2011;17(12):734-742. doi:10.1016/j.molmed.2011.07.008
- Lee WS, Baldassari S, Stephenson SEM, Lockhart PJ, Baulac S, Leventer RJ. Cortical dysplasia and the mTOR pathway: how the study of human brain tissue has led to insights into epileptogenesis. *Int J Mol Sci*. 2022;23(3):1344. doi:10.3390/ijms23031344
- Crino PB. Molecular pathogenesis of focal cortical dysplasia and hemimegalencephaly. *J Child Neurol*. 2005;20(4):330-336. doi:10.1177/08830738050200041101
- Gerasimenko A, Baldassari S, Baulac S. mTOR pathway: insights into an established pathway for brain mosaicism in epilepsy. *Neurobiol Dis*. 2023;182:106144. doi:10.1016/j.nbd.2023.106144
- Saxton RA, Sabatini DM. mTOR signaling in growth, metabolism, and disease. *Cell*. 2017;168(6):960-976. doi:10.1016/j.cell.2017.02.004
- Lee JH, Huynh M, Silhavy JL, et al. De novo somatic mutations in components of the PI3K-AKT3-mTOR pathway cause hemimegalencephaly. *Nat Genet*. 2012;44(8):941-945. doi:10.1038/ng.2329
- Leventer RJ, Scerri T, Marsh AP, et al. Hemispheric cortical dysplasia secondary to a mosaic somatic mutation in MTOR. *Neurology*. 2015;84(20):2029-2032. doi:10.1212/WNL.0000000000001594
- Nakashima M, Saito H, Takei N, et al. Somatic mutations in the MTOR gene cause focal cortical dysplasia type IIb. *Ann Neurol*. 2015;78(3):375-386. doi:10.1002/ana.24444
- Lim JS, Kim WI, Kang HC, et al. Brain somatic mutations in MTOR cause focal cortical dysplasia type II leading to intractable epilepsy. *Nat Med*. 2015;21(4):395-400. doi:10.1038/nm.3824
- Poduri A, Evrony GD, Cai X, et al. Somatic activation of AKT3 causes hemispheric developmental brain malformations. *Neuron*. 2012;74(1):41-48. doi:10.1016/j.neuron.2012.03.010
- Salinas V, Vega P, Piccirilli MV, et al. Identification of a somatic mutation in the RHEB gene through high depth and ultra-high depth next generation sequencing in a patient with hemimegalencephaly and drug resistant Epilepsy. *Eur J Med Genet*. 2019;62(11):103571. doi:10.1016/j.ejmg.2018.11.005
- D'Gama AM, Geng Y, Couto JA, et al. Mammalian target of rapamycin pathway mutations cause hemimegalencephaly and focal cortical dysplasia. *Ann Neurol*. 2015;77(4):720-725. doi:10.1002/ana.24357
- Lim JS, Gopalappa R, Kim SH, et al. Somatic mutations in TSC1 and TSC2 cause focal cortical dysplasia. *Am J Hum Genet*. 2017;100(3):454-472. doi:10.1016/j.ajhg.2017.01.030
- D'Gama AM, Woodworth MB, Hossain AA, et al. Somatic mutations activating the mTOR pathway in dorsal telencephalic progenitors cause a continuum of cortical dysplasias. *Cell Rep*. 2017;21(13):3754-3766. doi:10.1016/j.celrep.2017.11.106
- Jamar SS, Schmitz-Abe K, D'Gama AM, et al. Biallelic mutations in human DCC cause developmental split-brain syndrome. *Nat Genet*. 2017;49(4):606-612. doi:10.1038/ng.3804
- Mirzaa GM, Campbell CD, Solovieff N, et al. Association of mTOR mutations with developmental brain disorders, including megalencephaly, focal cortical dysplasia, and pigmentary mosaicism. *JAMA Neurol*. 2016;73(7):836-845. doi:10.1001/jamaneuro.2016.0363
- Scheffer IE, Heron SE, Regan BM, et al. Mutations in mammalian target of rapamycin regulator DEPDC5 cause focal epilepsy with brain malformations. *Ann Neurol*. 2014;75(5):782-787. doi:10.1002/ana.24126
- Child ND, Cascino GD. Mystery case: Cowden syndrome presenting with partial epilepsy related to focal cortical dysplasia. *Neurology*. 2013;81(13):e98-e99. doi:10.1212/WNL.0b013e3182a55ef0
- Adachi T, Takigawa H, Nomura T, Watanabe Y, Kowa H. Cowden syndrome with a Novel PTEN mutation presenting with partial epilepsy related to focal cortical dysplasia. *Intern Med*. 2018;57(1):97-99. doi:10.2169/internalmedicine.9052-17
- Baldassari S, Licchetta L, Tinuper P, Bisulli F, Pippucci T, GATOR1 complex: the common genetic actor in focal epilepsies. *J Med Genet*. 2016;53(8):503-510. doi:10.1136/jmedgenet-2016-103883
- Sim JC, Scerri T, Fanjul-Fernandez M, et al. Familial cortical dysplasia caused by mutation in the mammalian target of rapamycin regulator NPRL3. *Ann Neurol*. 2016;79(1):132-137. doi:10.1002/ana.24502
- Iffland PH 2nd, Crino PB. Focal cortical dysplasia: gene mutations, cell signaling, and therapeutic implications. *Annu Rev Pathol*. 2017;12:547-571. doi:10.1146/annurev-pathol-052016-100138
- Qin W, Chan JA, Vinters HV, et al. Analysis of TSC cortical tubers by deep sequencing of TSC1, TSC2 and KRAS demonstrates that small second-hit mutations in these genes are rare events. *Brain Pathol*. 2010;20(6):1096-1105. doi:10.1111/j.1750-3639.2010.00416.x
- Baulac S, Ishida S, Marsan E, et al. Familial focal epilepsy with focal cortical dysplasia due to DEPDC5 mutations. *Ann Neurol*. 2015;77(4):675-683. doi:10.1002/ana.24368
- Peloro C, Watrin F, Conti V, et al. Somatic double-hit in MTOR and RPS6 in hemimegalencephaly with intractable epilepsy. *Hum Mol Genet*. 2019;28(22):3755-3765. doi:10.1093/hmg/ddz194
- Sim NS, Ko A, Kim WK, et al. Precise detection of low-level somatic mutation in resected epilepsy brain tissue. *Acta Neuropathol*. 2019;138(6):901-912. doi:10.1007/s00401-019-02052-6
- Ribierre T, Deleuze C, Bacq A, et al. Second-hit mosaic mutation in mTORC1 repressor DEPDC5 causes focal cortical dysplasia-associated epilepsy. *J Clin Invest*. 2018;128(6):2452-2458. doi:10.1172/JCI99384
- Baldassari S, Ribierre T, Marsan E, et al. Dissecting the genetic basis of focal cortical dysplasia: a large cohort study. *Acta Neuropathol*. 2019;138(6):885-900. doi:10.1007/s00401-019-02061-5
- Marsan E, Baulac S. Review: mechanistic target of rapamycin (mTOR) pathway, focal cortical dysplasia and epilepsy. *Neuropathol Appl Neurobiol*. 2018;44(1):6-17. doi:10.1111/nan.12463
- Blumcke I, Thom M, Aronica E, et al. The clinicopathologic spectrum of focal cortical dysplasias: a consensus classification proposed by an ad hoc Task Force of the ILAE Diagnostic Methods Commission. *Epilepsia*. 2011;52(1):158-174. doi:10.1111/j.1528-1167.2010.02777.x
- Schur S, Moreau JT, Khoo HM, et al. New interinstitutional, multimodal presurgical evaluation protocol associated with improved seizure freedom for poorly defined cases of focal epilepsy in children. *J Neurosurg Pediatr*. 2022;29(1):74-82. doi:10.3171/2021.6.PEDS218
- Assessed July 20, 2023. bitbucket.org/muggic/muggic_pipelines
- Assessed July 20, 2023. gnomad.broadinstitute.org/
- Assessed July 20, 2023. cancer.sanger.ac.uk/cosmic
- Richards S, Aziz N, Bale S, et al. Standards and guidelines for the interpretation of sequence variants: a joint consensus recommendation of the American College of Medical Genetics and Genomics and the Association for Molecular Pathology. *Genet Med*. 2015;17(5):405-424. doi:10.1038/gim.2015.30
- Katz Y, Wang ET, Airolidi EM, Burge CB. Analysis and design of RNA sequencing experiments for identifying isoform regulation. *Nat Methods*. 2010;7(12):1009-1015. doi:10.1038/nmeth.1528
- Kim JK, Cho J, Kim SH, et al. Brain somatic mutations in MTOR reveal translational dysregulations underlying intractable focal epilepsy. *J Clin Invest*. 2019;129(10):4207-4223. doi:10.1172/JCI127032
- Lopez-Rivera JA, Leu C, Macnee M, et al. The genomic landscape across 474 surgically accessible epileptogenic human brain lesions. *Brain*. 2023;146(4):1342-1356. doi:10.1093/brain/awac376
- Moller RS, Weckhuysen S, Chipaux M, et al. Germline and somatic mutations in the MTOR gene in focal cortical dysplasia and epilepsy. *Neurol Genet*. 2016;2(6):e118. doi:10.1212/NXG.0000000000000118
- Wieser HG, Blume WT, Fish D, et al. Proposal for a new classification of outcome with respect to epileptic seizures following epilepsy surgery. *Epilepsia*. 2001;42(s2):282-286. doi:10.1046/j.1528-1157.2001.4220282.x
- Engel J Jr, Van Ness PC, Rasmussen TB, Ojemann LM. Outcome with respect to epileptic seizure. In: Jr IEJ, ed. *Surgical Treatment of the Epilepsies*. Raven Press; 1993:609-621.
- Chung C, Yang X, Bae T, et al. Comprehensive multi-omic profiling of somatic mutations in malformations of cortical development. *Nat Genet*. 2023;55(2):209-220. doi:10.1038/s41588-022-01276-9
- Morini A, Drossart T, Timsit MO, et al. Low-grade oncogenic renal tumor (LOT): mutations in mTOR pathway genes and low expression of FOXI1. *Mod Pathol*. 2022;35(3):352-360. doi:10.1038/s41379-021-00906-7
- Pirozzi F, Berkseth M, Shear R, et al. Profiling PI3K-AKT-MTOR variants in focal brain malformations reveals new insights for diagnostic care. *Brain*. 2022;145(3):925-938. doi:10.1093/brain/awab376

48. Lee WS, Stephenson SEM, Howell KB, et al. Second-hit DEPDC5 mutation is limited to dysmorphic neurons in cortical dysplasia type IIA. *Ann Clin Transl Neurol.* 2019; 6(7):1338-1344. doi:10.1002/acn3.50815
49. Yang H, Rudge DG, Koos JD, Vaidialingam B, Yang HJ, Pavletich NP. mTOR kinase structure, mechanism and regulation. *Nature.* 2013;497(7448):217-223. doi:10.1038/nature12122
50. Tripolszki K, Knox R, Parker V, et al. Somatic mosaicism of the PIK3CA gene identified in a Hungarian girl with macrodactyly and syndactyly. *Eur J Med Genet.* 2016;59(4):223-226. doi:10.1016/j.ejmg.2016.02.002
51. Moloney PB, Cavalleri GL, Delanty N. Epilepsy in the mTORopathies: opportunities for precision medicine. *Brain Commun.* 2021;3(4):fcab222. doi:10.1093/brain-comms/fcab222
52. Gao XH, Li J, Gong HF, et al. Comparison of fresh frozen tissue with formalin-fixed paraffin-embedded tissue for mutation analysis using a multi-gene panel in patients with colorectal cancer. *Front Oncol.* 2020;10:310. doi:10.3389/fonc.2020.00310
53. Arai H, Akagi K, Nakagawa A, et al. Clinical and genetic diagnosis of Cowden syndrome: a case report of a rare PTEN germline variant and diverse clinical presentation. *Medicine.* 2023;102(1):e32572. doi:10.1097/MD.00000000000032572